

## Monte Carlo study of the temperature dependence of domain-growth kinetics in a system with a nonconserved order parameter and a zero-temperature equilibration fixed point

Kristen A. Fichthorn

*Department of Chemical Engineering, 164 Fenske Laboratory, Pennsylvania State University,  
University Park, Pennsylvania 16802*

W. Henry Weinberg

*Department of Chemical Engineering, University of California, Santa Barbara, California 93106*  
(Received 27 November 1991; revised manuscript received 16 July 1992)

We have investigated the relationship between the proportionality factor in the Lifschitz-Allen-Cahn scaling relation and the microscopic kinetics of nonequilibrium transport in a Monte Carlo model of domain growth in a two-dimensional, quenched, chemisorbed overlayer with a nonconserved order parameter and a zero-temperature equilibration fixed point. We have identified two components of the proportionality factor, which reflect the two temperature dependences of domain growth in this system. The primary temperature dependence arises from the rate of surface diffusion. In addition, we find a factor,  $\alpha$ , which decreases with increasing temperature due to the influence of thermal fluctuations. We also find that the proportionality factor has a time dependence, which arises from the rate of surface diffusion. We have found that this time dependence can influence the apparent form of the growth law. We discuss why the observed time dependence of diffusion should be a general phenomenon present in both simulations and experiments of domain growth in quenched systems.

### I. INTRODUCTION

There has been widespread interest in the time evolution of disordered systems which are quenched to temperatures below the order-disorder phase transition temperature.<sup>1-34</sup> In these systems, the development of long-range order proceeds by the growth of ordered domains. It has been well established that growth in the late stages can be described by a simple power-law scaling of the characteristic domain length with time, i.e.,

$$l(t) \propto (At)^x, \quad (1)$$

where  $l(t)$  is a characteristic length of the domains at a time  $t$ ,  $x$  is the growth exponent, and  $A$  is a proportionality factor. For systems which do not conserve the order parameter, the scaling relation of Eq. (1) represents the Lifschitz-Allen-Cahn theory of curvature-driven growth,<sup>4,5</sup> in which  $x = \frac{1}{2}$ . Both computer simulations<sup>6-19</sup> and experiments<sup>20-22</sup> have verified the Lifschitz-Allen-Cahn growth law in many such systems.

From a microscopic perspective, domain growth is brought about by the complex, nonequilibrium diffusion of self-organizing species. Since the physics of curvature-driven growth is well understood from the macroscopic level, the proportionality factor of Eq. (1) can be taken as a measure of the transport phenomena which mediate growth. Numerical investigations<sup>16-19,23</sup> of domain growth at temperatures approaching zero have indicated that two types of behavior can exist in systems with a nonconserved order parameter: freezing or equilibrating. It is believed<sup>18,24</sup> that freezing or nonfreezing behavior has its origin in the detailed form of the proportionality factor and it has been suggested<sup>24</sup> that systems can be classified based upon the general form of  $A$ . In

the interest of gaining insight to possible generalities in the transport physics which characterize domain growth in freezing and nonfreezing systems, we have investigated the relationship between the proportionality factor for domain growth and the microscopic kinetics of transport in two Monte Carlo models of quenched, chemisorbed overlayers. One of these systems exhibits zero-temperature freezing<sup>25</sup> and, in the other, growth continues until thermal equilibrium is achieved. In this paper, we discuss the behavior of the system which equilibrates at 0 K. We find that the proportionality factor in this system can be expressed as a product of three factors, i.e.,

$$A = \kappa \alpha \Gamma. \quad (2)$$

Here,  $\kappa$  is a constant,  $\alpha$  models the effect of thermal fluctuations, and  $\Gamma$  is the rate of adatom hopping.

### II. MODEL

The model we consider is a two-dimensional, square-lattice gas with equal and repulsive nearest- and next-nearest-neighbor interactions and with conserved density. At a fractional coverage of  $\frac{1}{2}$ , the ground state of this system has  $(2 \times 1)$  ordering and is fourfold degenerate, as shown in Fig. 1. To simulate the kinetics in our studies, we adopted a model of precursor-mediated surface diffusion which was first utilized by Kang and Weinberg.<sup>14</sup> In a precursor-mediated surface diffusion, a chemisorbed particle is immobile until it is thermally excited into a physically adsorbed precursor state. In the precursor state, particles are less strongly bound than they are in the chemisorbed state, are weakly coupled to the lattice, and have a low-energy barrier to mobility. A particle which is physically adsorbed executes nearest-

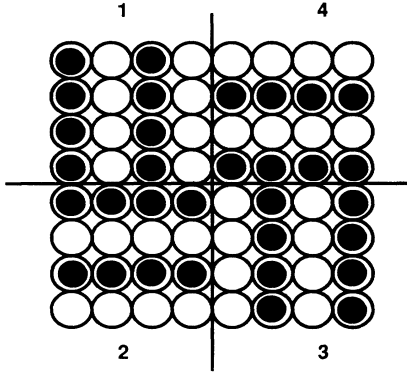


FIG. 1. The four, ordered  $(2 \times 1)$  ground-state configurations which are possible in a square-lattice gas with equal nearest- and next-nearest-neighbor repulsion below  $T_c$ .

neighbor hops from site to site (over both occupied and vacant sites) until it eventually deexcites at a vacant site into the chemisorbed state. The potential energy surface of the physically adsorbed precursor is taken to be periodic and uniform, in that locations above both chemisorbed species and vacant substrate sites are given equal energies. By contrast, the energy difference between a chemisorbed particle and its transition state is assumed to be given by

$$E_c(n) = E_{c,0} - n\phi, \quad (3)$$

where  $E_{c,0}$  is the potential energy of an isolated, chemisorbed particle,  $\phi$  is the pairwise-additive lateral interaction strength, and  $n$  is the total number of nearest- and next-nearest-neighbors surrounding a chemisorbed species. This feature of the model is intended to represent the effect of adsorbate interactions in altering the potential energy of chemisorbed species. Although, in principle, physically adsorbed particles could also interact with one another, we have chosen to model the situation in which the barrier to excitation is much greater than the barrier to deexcitation. The concentration of physically adsorbed precursors is negligible under these circumstances and their mutual interaction can be omitted.

The dynamics of precursor-mediated surface diffusion are modeled by 11 time scales of which 9 characterize excitation of a chemisorbed species to the physically adsorbed state,

$$\tau_{\text{ex}}^{-1} = \nu_{\text{l,ex}} e^{-E_c(i)/k_B T}, \quad i = 0, 8; \quad (4)$$

one characterizes deexcitation from the physically adsorbed state to the chemisorbed state,

$$\tau_{\text{dex}}^{-1} = \nu_{\text{l,dex}} e^{-E_{\text{dex}}/k_B T}, \quad (5)$$

and one characterizes the migration of a physically adsorbed precursor,

$$\tau_{\text{mig}}^{-1} = \frac{1}{4} \nu_{\parallel} e^{-E_{\text{mig}}/k_B T}. \quad (6)$$

We incorporated these time scales into a dynamical Monte Carlo algorithm designed to simulate the system

as a Poisson process.<sup>26</sup> Similar algorithms have been used in a few other studies of domain growth kinetics.<sup>14,27,28</sup> The key steps in the simulation algorithm are the following.

(1) On trial  $k$  at time  $t_k$ , the time scale of every possible excitation event on the lattice is calculated and the number  $m_{\text{ex},i}$  of possible events with a time scale  $\tau_{\text{ex},i}$  (or rate,  $r_{\text{ex},i} = \tau_{\text{ex},i}^{-1}$ ) is counted.

(2) The probability  $p_{\text{ex},i}$  of conducting an event of type  $i$  is determined as

$$p_{\text{ex},i} = \frac{m_{\text{ex},i} r_{\text{ex},i}}{\sum_j m_{\text{ex},j} r_{\text{ex},j}}. \quad (7)$$

(3) A group  $i$  is selected based on a comparison of its probability of excitation,  $p_{\text{ex},i}$ , to a generated uniform random number  $R \in (0, \dots, 1)$ .

(4) A particular excitation event in group  $i$  is selected randomly and time is incremented utilizing the fact that the mean interevent time in the simulated Poisson process is given by<sup>26</sup>

$$\tau = \frac{6}{\sum_j m_{\text{ex},j} r_{\text{ex},j}}. \quad (8)$$

To strictly satisfy the requirement for simulating a Poisson process, the time increment at each step should be selected from an exponential distribution with a mean given by Eq. (8). We incremented time at each step with the mean of the distribution. Over many trials and many different runs, a mean time increment, as given by Eq. (8), will arise in the more rigorous situation.

(5) Once a species has been excited to the physically adsorbed state, it performs a random walk consisting of nearest-neighbor hops until it deexcites at a vacant site. The random walk and eventual deexcitation of the precursor is simulated as follows.

(a) A random number,  $R \in (0, \dots, 1)$ , is generated.

(b) If  $R$  is less than the probability of deexcitation, then deexcitation is attempted and is successful if the particle is above a vacant site. Otherwise, a nearest-neighbor site (one of four possible for a square lattice) is chosen randomly and the particle is moved to that site. The probability of deexcitation,  $p_{\text{dex}}$ , is calculated via

$$p_{\text{dex}} = \frac{r_{\text{dex}}}{r_{\text{dex}} + 4r_{\text{mig}}}, \quad (9)$$

and the probability of migration is  $p_{\text{mig}} = 1 - p_{\text{dex}}$ .

(c) If a deexcitation event occurs, then the algorithm recommences with step (1). Otherwise, step (5) is repeated until deexcitation occurs.

Time in the algorithm is incremented only for excitations, reflecting that the time scales for excitation are significantly larger than those for deexcitation and migration. Compliance with the Poisson process would imply that, once an excitation event is chosen, the time increment should be

$$\tau = \frac{6}{\sum_{j=1}^M r_{\text{ex},j}^{-1} + r_{\text{dex}} + 4r_{\text{mig}}}, \quad (10)$$

where  $M$  is the total number of particles in the system.

However, if  $r_{\text{dex}} + 4r_{\text{mig}} \gg \sum r_{\text{ex},j}$ , then the time increment once particles are in the excited state becomes very small compared to the increment when no particles are excited. In addition, the probability of exciting another particle to the physically adsorbed state will be small, motivating the sequence of alternating excitations and deexcitations on a finite lattice.

Relevant parameters in this model are the activation energies and preexponential factors for excitation, deexcitation, and migration, which were chosen to be  $E_{c,0} = 8\phi$ ,  $E_{\text{dex}} = \phi = E_{\text{mig}}$ , and  $v_{\perp,\text{ex}} = v_{\perp,\text{dex}} = v_{\parallel}$ . With  $E_{\text{dex}} = E_{\text{mig}}$ , it can be shown that the statistical properties of the physically adsorbed random walker are independent of temperature.<sup>14</sup> Hence, in this work, the effect of the random walker on the proportionality factor was identical at all temperatures. Simulations were run at temperatures of  $k_B T = 0.1\phi, 0.25\phi, 0.3325\phi, 0.35\phi, 0.40\phi$ , and at a temperature arbitrarily close to zero to verify the equilibrating behavior of the system. At each temperature, 15–20 runs were conducted on  $400 \times 400$  and  $512 \times 512$  ( $k_B T/\phi = 0.10, 0.25$ , and  $0.40$ ) square lattices with periodic boundary conditions. The initial lattice was randomly populated with particles at a fractional coverage of  $\frac{1}{2}$  in all simulations. At periodic intervals during a simulation run, the average size of the domains was measured and recorded. We found that, by including as part of a domain only those particles having all eight nearest and next-nearest neighbors consistent with the  $(2 \times 1)$  pattern, fluctuations in the measured average domain area as a function of time could be significantly reduced. In light of previously reported difficulties with the quality of random numbers in this application,<sup>29</sup> special attention was given to assure the effective randomness of the pseudorandom numbers.

During a simulation run, time was incremented, upon the excitation of a chemisorbed particle, in both “real-time” units [i.e., as given by Eq. (8)], and in units of “uniform interevent steps” (UIS), in which  $1 \text{ UIS} = 1/N\theta$  ( $N = 400^2$  or  $512^2$ ). By incrementing time in uniform units of UIS and only upon the realization of an event, we eliminate all possible time and temperature dependencies of domain growth which would arise in the simulated rate of surface diffusion. In a previous study,<sup>10</sup> we showed that UIS could be used to overcome the influence of “initial transients” in Monte Carlo simulations of domain growth. Here, we use this method to provide a resolution of the transport physics contained in  $A$ .

### III. RESULTS AND DISCUSSION

Figure 2 shows log-log plots of the average linear dimension of a domain,  $\langle l \rangle$ , in units of the lattice constant,  $\lambda$ , as a function of UIS,  $U$ , for  $k_B T/\phi = 0.10$  [Fig. 2(a)] and the highest [ $k_B T/\phi = 0.40$ , Fig. 2(b)] temperature probed in this study. The results of all simulation runs at these temperatures are shown. It can be seen in Fig. 2 that the slopes of the curves attain approximate values of  $\frac{1}{2}$  at long times. Measured slopes at all temperatures were the following:  $0.478 \pm 0.002$  ( $k_B T/\phi = 0.10$ ),  $0.500 \pm 0.001$  ( $k_B T/\phi = 0.25$ ),  $0.482 \pm 0.002$  ( $k_B T/\phi = 0.3325$ ),  $0.481 \pm 0.006$  ( $k_B T/\phi = 0.35$ ), and

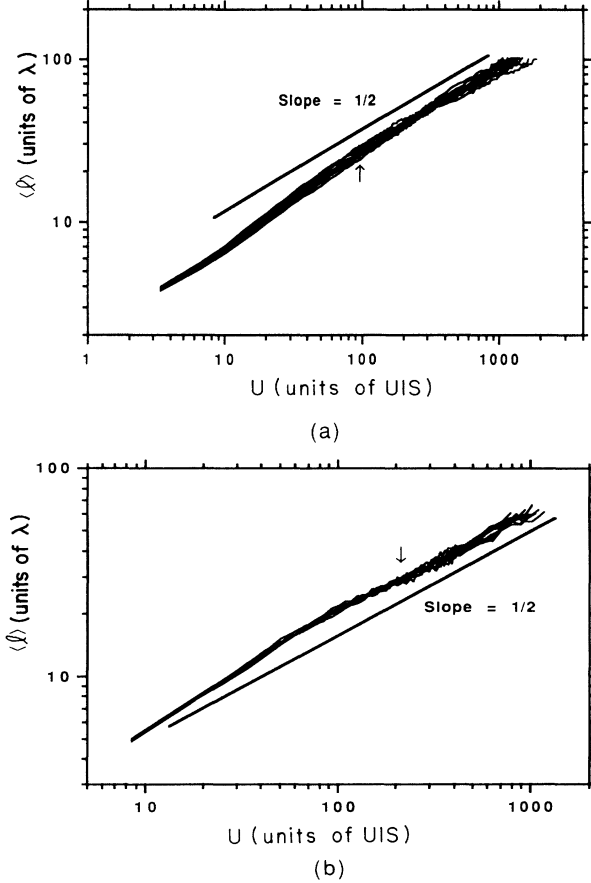


FIG. 2. Logarithmic plots of the average domain size  $\langle l \rangle$  as a function of UIS-time,  $U$ , at (a)  $k_B T/\phi = 0.10$  and (b)  $k_B T/\phi = 0.40$ . Lines with slopes of  $\frac{1}{2}$  are included for comparison. The results at times greater than those indicated by the arrows were utilized to estimate the asymptotic values of the growth exponents.

$0.480 \pm 0.005$  ( $k_B T/\phi = 0.40$ ). The uncertainties are one standard deviation in a linear least-squares fit of the data. At a given temperature, fits were obtained utilizing the results of all runs as “one big run.” Graphs were matched to a line with a slope of  $\frac{1}{2}$  and domain sizes which reflected true asymptotic behavior were utilized in the fit, as indicated by the arrows in Fig. 2. In some of the simulation runs on  $400 \times 400$  lattices, finite size effects became prominent in the late stages of growth. Hence, we excluded these results from the analysis.

It can be seen in Fig. 2 that the asymptotic scaling regime was initially reached at smaller domain sizes as the quench temperature was increased. In addition, more UIS were necessary to achieve a domain of a given size at high temperatures than at low temperatures. For example, at  $k_B T/\phi = 0.10$ , approximately 400 UIS are necessary to achieve an average domain size of  $50\lambda$ , while at  $k_B T/\phi = 0.40$ , about twice as many UIS were required to achieve the same average size. This trend is reflected in the proportionality factors, which are scaled and shown in Fig. 3. The error bars in Fig. 3 were derived from a standard error propagation analysis utilizing the errors in

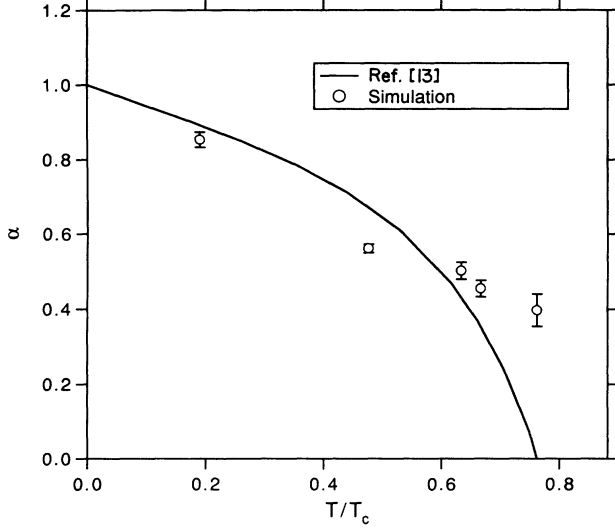


FIG. 3. The factor  $\alpha$  contains the temperature dependence of domain growth which can be attributed to the effects of thermal fluctuations. Here, we compare the values of  $\alpha$  obtained from our simulations to a theoretical form predicted by Grant and Gunton (Ref. 31) (see text). The uncertainty in  $\alpha$  was determined by a standard error propagation analysis given the errors in the slopes and intercepts of the fitted logarithmic  $\langle l \rangle$  vs  $U$  curves at each temperature. The simulation values of  $\alpha$  were scaled by a factor of  $\frac{1}{13}$  to match the theoretical expression. The simulation temperatures were also scaled by  $k_B T_c / \phi = 0.525$ .<sup>32</sup>

the slopes and intercepts of the fitted  $\log \langle l \rangle$  vs  $\log U$  curves.

It should be stressed that, by incrementing time in UIS, as described above, we simulate a system in which the rate of excitation is a constant and independent of temperature. Hence, the variation of the proportionality factor with temperature reflects a change in the efficiency of growth. It is expected<sup>7,8,30,31</sup> that thermal fluctuations in domain growth should become increasingly prominent at temperatures approaching  $T_c$ . These fluctuations slow the rate of growth and, eventually, prevent it above  $T_c$ . Theories of domain growth which include thermal fluctuations have been developed for the antiferromagnetic Ising model.<sup>7,30,31</sup> These theories predict that the slowing of domain growth arises through the proportionality factor, which can be expressed by the form given in Eq. (2). Considering thermal fluctuations as the origin of the observed slowing down of growth, we compared the proportionality factors from our simulations to an expression derived by Grant and Gunton<sup>31</sup> for the temperature dependence of  $\alpha$  [cf. Eq (2)] in the antiferromagnetic Ising model. This expression has the analytical form

$$\alpha = 1 - (k_B T / \sqrt{\pi} \sigma \omega) n, \quad (11)$$

where the Onsager solution for the surface tension,  $\sigma$ , is given by

$$\sigma \lambda = 2\phi \left[ 1 - \frac{k_B T}{2\phi} \ln \coth \left( \frac{\phi}{k_B T} \right) \right]. \quad (12)$$

Here,  $\omega$  is the thickness of the interface,  $\lambda$  is the lattice constant, and  $n$  is a parameter with a value close to unity. For comparison to our results, we chose the ratio  $n/\omega$  in this expression to be  $\sqrt{\pi}/2\lambda$ . This value of  $n/\omega$  gave a satisfactory fit of our results to Eq. (11) and it is a physically reasonable estimate of the width of a domain boundary with  $n$  on the order of unity. Larger values of  $n/\omega$  in Eq. (11) yield a steeper slope in the low-temperature region of the curve. In addition, the theoretical expression of Eq. (11) goes to zero at lower temperatures for larger ratios of  $n/\omega$ . The proportionality factors shown in Fig. 3 were multiplied by a factor of  $\frac{1}{13}$  to scale our results to those of Grant and Gunton. This factor should be equated to  $\kappa$  in Eq. (2). To scale the temperatures, we utilized the value  $k_B T_c / \phi = 0.525$ , as indicated by Binder and Landau.<sup>32</sup> Although Eqs. (11) and (12) were derived for the Ising model with nearest-neighbor interactions, we observed reasonable agreement between our results and the expression of Grant and Gunton at temperatures below approximately  $0.65 T_c$ .

In Fig. 4, the average domain sizes,  $\langle l \rangle$ , as a function

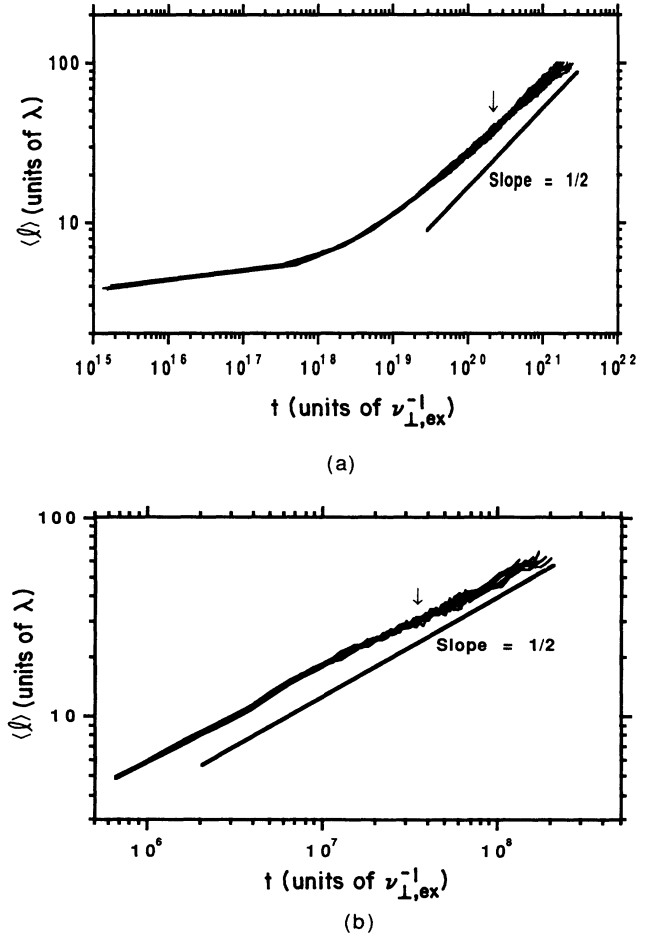


FIG. 4. Logarithmic plots of the average domain size  $\langle l \rangle$  as a function of real-time,  $t$ , at (a)  $k_B T / \phi = 0.10$  and (b)  $k_B T / \phi = 0.40$ . Lines with known slopes of  $\frac{1}{2}$  are included for comparison. The results at times greater than those indicated by the arrows were utilized to estimate the asymptotic values of the growth exponents.

of real time,  $t$ , are shown for  $k_B T/\phi=0.10$  [Fig. 4(a)] and the highest [Fig. 4(b)] temperature probed in this study. As in Fig. 2, the results of all runs at these temperatures are shown. A comparison of Figs. 2(a) and 4(a) reveals that, while the slopes of the  $\log\langle l \rangle$  vs  $\log U$  curves decrease to an asymptotic value of  $\frac{1}{2}$  from an initially higher value, the slopes of the  $\log\langle l \rangle$  vs  $\log t$  curves increase with time toward a value of  $\frac{1}{2}$ . This behavior was characteristic of the runs conducted at lower temperatures. As the quench temperature of the system approached  $T_c$ , we found that there was less disparity between the UIS- and real-time plots. A comparison of Figs. 2(b) and 4(b) shows that, at  $k_B T/\phi=0.40$ , the UIS-time and real-time plots are very similar. This effect arises from the time and temperature dependence of our simulated rate of surface diffusion.

An appraisal of the time dependence of the simulated rate of excitation at varying temperatures can be obtained through examination of the relationship between the UIS- and real-time increments, given by<sup>10</sup>

$$\Gamma(t)dt = dU. \quad (13)$$

In Fig. 5, we show two log-log plots of the derivative of

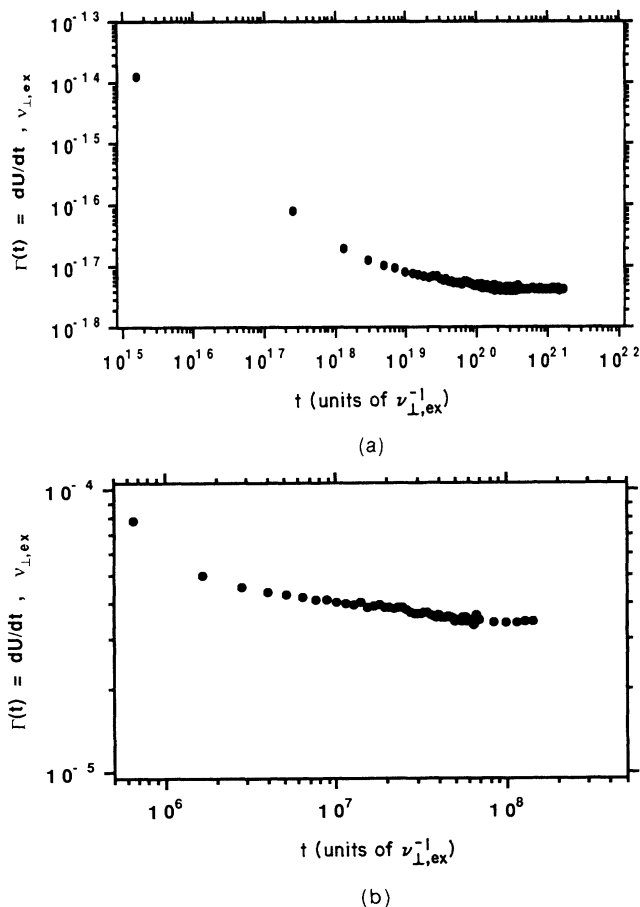


FIG. 5. The derivative of UIS time,  $U$ , with respect to real time,  $t$ , shown for two representative runs at (a)  $k_B T/\phi=0.10$  and (b)  $k_B T/\phi=0.40$ . The time dependence of the rate of particle excitation,  $\Gamma(t)$ , is given by these curves, as indicated by Eq. (13).

UIS time with respect to real time as a function of real time for representative runs at  $k_B T/\phi=0.10$  [Fig. 5(a)] and  $k_B T/\phi=0.40$  [Fig. 5(b)]. The time dependence of the rate of particle excitation,  $\Gamma$ , is given by these curves. At  $k_B T/\phi=0.10$ ,  $\Gamma$  decreases by over three orders of magnitude and appears to reach an effectively constant value at long times. The decrease in  $\Gamma$  was not nearly so dramatic—less than one order of magnitude—at  $k_B T/\phi=0.40$ . The time dependence of  $\Gamma$  can be understood in terms of a change in the distribution of particle energies (i.e., excitation rates) with time. Immediately subsequent to the quench, the system is at an energy consistent with an infinite temperature and the rate of particle excitation is large. As the system approaches thermodynamic equilibrium, its energy decreases and there is a corresponding decrease in the rate of particle excitation [cf. Eq. (8)]. Differences in the time dependence of  $\Gamma$  at different temperatures occur because the rates of excitation have more distinct values at low temperatures than at high temperatures. Although surface diffusion is not represented explicitly in most Monte Carlo studies of domain growth, these simulations implicitly include some form of a time-dependent spin-flip/exchange rate which arises through the use of Monte Carlo steps (MCS). The MCS is a time increment measuring transition attempts. Initially, when the energy of the system is high, transitions occur relatively frequently and the relative success-to-attempt ratio is high. As the system approaches thermal equilibrium, an increasing number of attempts are necessary to achieve a successful transition. The associated decrease in the rate of domain growth should be equated with a time dependence of the rate of mass transfer.

Strictly speaking,  $\Gamma$  will decrease continually until thermal equilibrium is achieved. However, it is possible, in the very late stages of growth, that  $\Gamma$  changes very slowly and can be considered to be effectively constant. If this condition is achieved, then Monte Carlo simulations will conform to theories of domain growth, which assume that  $\Gamma$  is constant. In our studies, we found that  $\Gamma$  did not reach a constant value at all of the temperatures for the times that we were able to follow. Moreover, in many of the runs,  $\Gamma$  became effectively constant only at very long times, leaving an inadequate time interval for reliable statistics. Both of these aspects are reflected in the measured slopes of the  $\log\langle l \rangle$  vs  $\log t$  curves, which were  $0.455 \pm 0.002$  ( $k_B T/\phi=0.10$ ),  $0.431 \pm 0.002$  ( $k_B T/\phi=0.25$ ),  $0.462 \pm 0.003$  ( $k_B T/\phi=0.3325$ ),  $0.466 \pm 0.004$  ( $k_B T/\phi=0.35$ ), and  $0.470 \pm 0.001$  ( $k_B T/\phi=0.40$ ). Analysis of the real-time curves was conducted in the same way as for the UIS-time results. The low values of the slopes arise from the time dependence of our simulated adatom hopping mechanism.<sup>10</sup>

Interestingly, we found that some of the logarithmic  $\langle l \rangle$  vs  $t$  curves attained slopes of  $\frac{1}{2}$  at short times. These, then, exhibited a decline in the slope followed by an eventual increase in the slope towards an asymptotic value of  $\frac{1}{2}$ . This was prevalent at temperatures above  $k_B T/\phi=0.25$ , and can be seen in Fig. 4(b). We view the early slope of  $\frac{1}{2}$  as a “false slope” because it arises as a

balance of the initial, transient acceleration of the growth rate [cf. Fig. 2] and the initial, transient decrease in the rate of adatom hopping (cf. Fig. 5). A similar effect has been noted by others<sup>15</sup> and has been attributed to "initial transients." We have shown<sup>10</sup> that these initial transients arise from the time dependence of simulated mass transfer kinetics.

It is possible that the type of behavior we have observed in this model is prevalent in experimental studies of domain growth in chemisorbed overlayers. Although it is debatable whether the exact mechanism of diffusion which we have simulated is widespread in chemisorbed overlayers, our model does capture the essential physics of an initially disordered, quenched, chemisorbed overlayer approaching thermal equilibrium. It is reasonable to expect a decrease in the rate of adatom hopping with time in this situation because experimental systems also conform to the detailed balance criterion which links kinetics with energy. As a quenched system reaches thermal equilibrium and decreases its energy, the overall rate of adatom hopping must also decrease. Our studies have shown that the rate at which the rate of adatom hopping decreases with time can significantly alter the apparent form of the asymptotic growth law.<sup>10</sup> In a model having the same Hamiltonian as this study, but utilizing a vacancy-mediated mechanism of surface diffusion, we found that  $\Gamma$  decreased very slowly with time.<sup>10</sup> We showed that the time dependence of  $\Gamma$  led to apparent growth laws of the Lifschitz-Slyozov<sup>33</sup> form [in which  $l(t) \sim t^{1/3}$ ] when, in fact, Lifschitz-Allen-Cahn growth was occurring.<sup>10</sup> It is certainly possible that the low growth exponents measured in experimental systems,<sup>34</sup> where the order parameter is presumably nonconserved, could reflect this influence. Since measured values of the growth exponents could reflect the time dependence of  $\Gamma$ ,

it is also unclear whether intercepts resulting from the analysis of logarithmic plots will provide a reliable measure of the energy barrier to surface diffusion.

#### IV. CONCLUSIONS

In summary, we have investigated and obtained a detailed resolution of the proportionality factor for domain growth in a Monte Carlo model of a two-dimensional, quenched, chemisorbed overlayer with a nonconserved order parameter and a zero-temperature equilibration fixed point. We have determined that the proportionality factor is comprised of two temperature-dependent factors: one,  $\Gamma$ , arising from the kinetics of surface diffusion and another,  $\alpha$ , from the effects of thermal fluctuations. Hence, the proportionality factor in our system is of the form given by Eq. (2). We find that the rate of surface diffusion decreases with time in this model and we conclude that this should be a general phenomenon, prevalent in both simulations and experimental studies of domain growth in quenched systems. We also conclude that the time dependence of surface-diffusion kinetics could be responsible for the low-growth exponents which have arisen in experimental studies of nonconserved systems.<sup>34</sup> It will be interesting to see whether our results for this system are of a general nature for nonfreezing, nonconserved systems and to contrast our findings to results for a freezing system.

#### ACKNOWLEDGMENTS

This work was supported under the National Science Foundation under Grant No. CHE-9003553 (W.H.W.) and Grant No. CTS-9058013 (K.A.F.). One of us (K.A.F.) also acknowledges support from IBM.

<sup>1</sup>*Dynamics of Ordering Processes in Condensed Matter*, edited by S. Komura and H. Furukawa (Plenum, New York, 1988).

<sup>2</sup>*Kinetics of Ordering and Growth at Surfaces*, edited by M. G. Lagally (Plenum, New York, 1989).

<sup>3</sup>*Phase Transitions and Critical Phenomena*, edited by C. Domb and J. L. Lebowitz (Academic, New York, 1983), Vol. 8.

<sup>4</sup>I. M. Lifschitz, *Zh. Eksp. Teor. Fiz.* **42**, 1354 (1962) [*Sov. Phys. JETP* **15**, 939 (1962)].

<sup>5</sup>S. M. Allen and J. W. Cahn, *Acta Metall.* **27**, 1085 (1979).

<sup>6</sup>Many references to numerical simulations can be found in the paper by G. F. Mazenko, *Phys. Rev. B* **43**, 8204 (1991).

<sup>7</sup>P. S. Sahni, G. S. Grest, and S. A. Safran, *Phys. Rev. Lett.* **50**, 60 (1983).

<sup>8</sup>K. Kaski, M. C. Yalabik, J. D. Gunton, and P. S. Sahni, *Phys. Rev. B* **28**, 5263 (1983).

<sup>9</sup>G. S. Grest, M. P. Anderson, and D. J. Srolovitz, *Phys. Rev. B* **38**, 4752 (1988).

<sup>10</sup>K. A. Fichthorn and W. H. Weinberg, *Phys. Rev. Lett.* **68**, 604 (1992).

<sup>11</sup>J. G. Amar, F. E. Sullivan, and R. D. Mountain, *Phys. Rev. B* **37**, 196 (1988).

<sup>12</sup>H. C. Fogedby and O. G. Mouristen, *Phys. Rev. B* **37**, 5962 (1988).

<sup>13</sup>A. Høst-Madsen, P. J. Shah, T. V. Hansen, and O. G. Mour-

isten, *Phys. Rev. B* **36**, 2333 (1987).

<sup>14</sup>H. C. Kang and W. H. Weinberg, *Phys. Rev. B* **41**, 2234 (1990).

<sup>15</sup>K. Kaski, S. Kumar, J. D. Gunton, and P. A. Rikvold, *Phys. Rev. B* **29**, 4420 (1984).

<sup>16</sup>A. Sadiq and K. Binder, *J. Stat. Phys.* **35**, 517 (1984).

<sup>17</sup>H. C. Kang, W. H. Weinberg, and M. W. Deem, *Phys. Rev. B* **43**, 11438 (1991).

<sup>18</sup>J. Viñals and J. D. Gunton, *Phys. Rev. B* **33**, 7795 (1986).

<sup>19</sup>J. Viñals and M. Grant, *Phys. Rev. B* **36**, 7036 (1987).

<sup>20</sup>G. C. Wang and T.-M. Lu, *Phys. Rev. Lett.* **50**, 2014 (1983).

<sup>21</sup>P. K. Wu, J. H. Perepezko, J. T. McKinney, and M. G. Lagally, *Phys. Rev. Lett.* **51**, 1577 (1983).

<sup>22</sup>J.-K. Zuo, G.-C. Wang, and T.-M. Lu, *Phys. Rev. B* **39**, 9432 (1989).

<sup>23</sup>H. C. Kang and W. H. Weinberg, *Phys. Rev. B* **40**, 7059 (1989).

<sup>24</sup>Z. W. Lai, G. F. Mazenko, and O. T. Valls, *Phys. Rev. B* **37**, 9481 (1988).

<sup>25</sup>K. A. Fichthorn and W. H. Weinberg (unpublished).

<sup>26</sup>K. A. Fichthorn and W. H. Weinberg, *J. Chem. Phys.* **95**, 1090 (1991).

<sup>27</sup>H. C. Kang and W. H. Weinberg, *J. Chem. Phys.* **90**, 2824 (1989).

- <sup>28</sup>H. C. Kang and W. H. Weinberg, *Phys. Rev. B* **38**, 11 543 (1988).
- <sup>29</sup>A. Milchev, K. Binder, and D. W. Heerman, *Z. Phys. B* **63**, 521 (1986).
- <sup>30</sup>S. A. Safran, P. S. Sahni, and G. S. Grest, *Phys. Rev. B* **28**, 2693 (1983).
- <sup>31</sup>M. Grant and J. D. Gunton, *Phys. Rev. B* **28**, 5496 (1983).
- <sup>32</sup>K. Binder and D. P. Landau, *Phys. Rev. B* **21**, 1941 (1980).
- <sup>33</sup>I. M. Lifschitz and V. V. Slyozov, *J. Chem. Phys. Solids* **15**, 35 (1961).
- <sup>34</sup>P. K. Wu, M. C. Tringides, and M. G. Lagally, *Phys. Rev. B* **39**, 7595 (1989).